Mixed Dual Finite Element Methods for the Treatment of Hexagonal Geometries in Diffusion Equations

Didier Schneider, Jean-Jacques Lautard
Commissariat à l'Energie Atomique
DEN/DM2S/SERMA
CEA SACLAY
91191 Gif sur Yvette Cedex France
didier.schneider@cea.fr
jean-jacques.lautard@cea.fr

Keywords : Diffusion, hexagonal, mixed finite elements, quadrangular, 2D mapping

Abstract

The mixed dual finite element method has been applied successfully to the treatment of 3D diffusion and simplified transport equations for Cartesian geometries. A specific solver known as MINOS, based on this method, has been implemented in the CRONOS code developed at the French Atomic Energy Commission (CEA). This solver produces very fast calculations due to discretization on a Raviart-Thomas-Nedelec (RTN) finite element basis, which generates well-structured and well-conditioned matrices. This method has recently been extended to hexagonal geometries by preserving its main feature. Different numerical approaches have been analyzed and compared and numerical results are presented on a standard benchmark problem.

1 Introduction

The CRONOS code (Lautard, 1990) is the computer tool devoted to core computation in the SAPHYR system. Within CRONOS, the MINOS solver is used to carry out fast homogenized core calculations for rectangular geometry. The first version of the MINOS solver (Lautard, 1993 and Lautard, 1994) was limited to the treatment of diffusion equations in Cartesian geometry, and it was extended to solve simplified P_N equations (Baudron 2001, Lautard, 1999). More recently, the solver has been extended to treat kinetic equations (Baudron, 2001). The latest improvement concerns hexagonal geometry and has been made in the general context of quadrangular geometry (Schneider, 2000).
In neutronics, the conventional finite element approach to solving the diffusion equation is to rewrite the problem in primal or hybrid primal variational form (Lewis, 1985, Palmiotti, 1993). The equation is then written using flux as the main unknown and the functional reads-in gradient operator terms. This approach is well suited to performing calculations on unstructured grids and also for parallel calculations. Nevertheless, we usually obtain unstructured matrices that penalize the computing time of the iterative solver. In the dual variational formulation, the functional is written taking current as the main unknown and the functional reads-in divergence operator terms. This method is of standard use in structural mechanics and also in fluid dynamics. In the particular case of rectangular geometries, the Raviart-Thomas-Nedelec finite element family (Raviart, 1977) produces nice structured sparse linear systems. A specific block Gauss-Seidel method on the three

components of the current vector has been implemented. This method can be viewed as an alternating direction method and is rapidly converging. Contrary to the primal approximation, flux can be discontinuous at the element interfaces. This gives more flexibility for following the large variation in flux level which is located between uranium and MOX assemblies in the LWR reactor devoted to fuel recycling. The solver has been coded to reach convergence either by refining the mesh size (*h*-convergence) or by increasing the degree of the element (*p*-convergence).

The good results which have been obtained with the Cartesian solver encourage us to extend its capabilities to hexagonal geometries, keeping the same powerful iterative algorithm. Unfortunately, its efficient numerical implementation is not straightforward. Most of the orthogonality properties of the Cartesian RTN bases are lost in a hexagonal situation. For this reason, several possibilities have been investigated, depending on how the hexagon is split into elementary sub-domains and what transformation is used from a reference element. The first idea has been to divide the hexagons into 6 triangles and to extend the RTN bases to equilateral triangles (Brezzi, 1991). A prototype code has shown that this method is not efficient, mainly because the iterative procedure requires double sweeping of the nodes for each of the 3 main axes of the geometry.

The recent works of Chao and Tsoulfanidis (Chao, 1995) on a nodal solver using a conformal mapping encourage us to extend this method to mixed dual finite elements. Unfortunately, this method has been rejected due to difficulties in meeting the interface boundary conditions. Another possibility is to extend the method proposed by Hennart Mund and Del-Valle (Hennart, 1997). They split a hexagon into four trapezoids and use a bilinear transformation of the trapezoids into rectangles. Contrary to Chao's method, the mapping is no longer conformal and the diffusion operator is no longer preserved. These methods have been extended to the mixed dual method satisfactorily. The main disadvantage is that it is complex to divide the trapezoid into smaller elements, thus achieving mesh convergence.

Finally, we have experimented with two new approaches consisting in splitting into three lozenges. The lozenges are transformed into rectangles by either affine mapping or conformal mapping. The advantage here is that each lozenge can be easily split into smaller lozenges, so there is no difficulty in obtaining convergence in space. By using RTN elements, we obtain well-structured matrices. Another advantage of this method is that it preserves the fundamental symmetries of the hexagonal geometry.

The paper is divided into 7 chapters. First, we review the standard mixed dual formulation of the diffusion operator, then we present the general framework of the geometrical transformations of the plane applied to the mixed dual variational formulation. The next chapter is a brief description of the existing Cartesian solver, and the main part of the paper is a description of the various possibilities we have explored for the hexagonal geometry. The following chapter is devoted to our recent work on the treatment of pin-by-pin hexagonal geometries. The last chapter describes a numerical application and a comparison of the different solutions on a standard Benchmark.

2 The mixed dual variational formulation

First and for the sake of simplicity, we consider the diffusion equation. This equation couples scalar flux ϕ with current $\vec{p}$; in each energy group, we have:

$$\begin{cases} \vec{\nabla}.\vec{p} + \Sigma\phi = S \\ \vec{\nabla}\phi + \mathrm{D}^{-1}\vec{p} = 0 \end{cases} \qquad \text{on } \Omega \subset \mathbb{R}^{\mathrm{d}} \tag{1}$$

By splitting the boundary into three parts $\Gamma_1 \cup \Gamma_2 \cup \Gamma_3 = \partial\Omega$ and by denoting β the monoenergetic albedo coefficient ($\beta \in]-1, +1[$), the boundary conditions can be written in a general form:

$$\begin{cases} \phi = 0 & \text{on } \Gamma_1 \quad (\text{ Dirichlet }) \\ \vec{p}.\vec{n} = 0 & \text{on } \Gamma_2 \quad (\text{ Neuman }) \\ \vec{p}.\vec{n} = \tau\phi \quad (\tau = \frac{1}{2}\frac{1-\beta}{1+\beta}) & \text{on } \Gamma_3 \quad (\text{ Robin }) \end{cases} \tag{2}$$

By projecting Eq. (1) and using the Green formula on the second equation, we get the weak mixed dual formulation; find $(\vec{p}, \phi) \in H_{0,\Gamma_2}(div, \Omega) \times L^2(\Omega)$ such that:

$$\begin{cases} \int_\Omega \mathrm{D}^{-1}\vec{p}.\vec{q}\,dx - \int_\Omega \phi\,\vec{\nabla}.\vec{q}\;dx + \int_{\Gamma_3} \frac{1}{\tau}(\vec{p}.\vec{n})(\vec{q}.\vec{n})d\gamma = 0 & \forall \vec{q} \in H_{0,\Gamma_2}(div, \Omega) \\ -\int_\Omega \vec{\nabla}.\vec{p}\,\psi\,dx - \int_\Omega \Sigma\phi\psi dx = -\int_\Omega S\psi dx & \forall \psi \in L^2(\Omega) \end{cases} \tag{3}$$

where $H_{0,\Gamma_2}(div, \Omega) = \left\{ \vec{p} \in [L^2(\Omega)]^d : \vec{\nabla}.\vec{p} \in L^2(\Omega) \text{ and } \vec{p}.\vec{n} = 0 \text{ on } \Gamma_2 \right\}$

One advantage of the dual method is that the discontinuity conditions (between fluxes at interfaces) can be introduced in a natural way into the functional subspaces (non-essential conditions) (Lautard, 1993).

2.1 General framework on arbitrary triangulation

Finite element discrete spaces are always associated with triangulation over the computational domain. The triangulation is composed of the union of polyhedra which can be of arbitrary shape. At all events, these arbitrary elements *K* are obtained as an image by a mapping F_K of a reference element $\hat{K}$. For instance, if the domain consists of the union of quadrilaterals (in 2D), the reference element can be the unit square. In this chapter, our intention is to have another point of view on the finite element problem by considering the problem as it can be written in the reference domain by the reciprocal of all the elementary mappings F_K. Our intention is thus to build a new reference variational problem defined on the reference domain.

Let $\overline{\Omega} = \bigcup_{K \in \mathrm{T_h}} K$ be a triangulation defined on the computational domain, and we denote by *G* the global mapping induced by the inverse of union of all elementary element mappings

$$G(x) = F_K^{-1}(x) \quad \text{if } x \in K \tag{4}$$

It can easily be shown that *G* defines a mapping from the computational domain into the reference domain $\overline{\hat{\Omega}} = G(\overline{\Omega})$.

In order to define a new variational mixed dual problem in the reference domain, and the associated functional spaces, we have to first introduce local isomorphisms on each of the two fundamental spaces $L^2(K)$ and $H(div,K)$.

In the sequel for each element *K*, we will denote by $DF = DF(\hat{x})$ the Jacobian matrix (for simplicity, we will drop the index *K* from now on), by $J = J(\hat{x}) = |\det(DF)|$ the Jacobian and by $J_n = J_n(\hat{x}) = J\left|(DF)^{-T}\hat{\vec{n}}\right|$ the surface Jacobian ($\hat{\vec{n}}$ being the unit outer normal vector). We also suppose afterwards that the local transformations are C^1-diffeomorphisms.

2.1.1 Local isomorphism of functional spaces

We first have to define two different isomorphisms for the scalar and vector functions. First, for all function $\hat{\phi}: K \to \mathbb{R}$, we associate the function $\phi = \mathbf{F}(\hat{\phi}): K \to \mathbb{R}$ defined by:

$$\phi = \hat{\phi} \circ F^{-1} \tag{5}$$

Application **F** defines an isomorphism from $H^1(\hat{K})$ to $H^1(K)$.

A similar transformation is not so straightforward for the vector space $H(div,K)$. In fact, the transformation, which, for a vectorial function $\hat{\vec{q}}: \hat{K} \to \mathbb{R}^d$, associates the vectorial function $\vec{q} = \hat{\vec{q}} \circ F^{-1}: K \to \mathbb{R}^d$, is not an isomorphism from $H(div,\hat{K})$ to $H(div,K)$. The adequate isomorphism has been used by Thomas and is known in the literature as the Piola transformation (Brezzi 1995).

At each vector function, $\hat{\vec{q}}: \hat{K} \to \mathbb{R}^d$, we associate a new vector by:

$$\vec{q} = \mathbf{G}(\hat{\vec{q}}) = \frac{1}{J}(DF)\hat{\vec{q}} \circ F^{-1}: K \to \mathbb{R}^d \tag{6}$$

Moreover, we have the following identity:

$$\forall \psi \in L^2(K), \forall \vec{q} \in H(div,K) \quad \int_K div\,\vec{q}\,\psi\,dx = \int_{\hat{K}} div\,\hat{\vec{q}}\,\hat{\psi}\,d\hat{x} \tag{7}$$

The two previous isomorphisms are not enough to write the reference mixed dual variational problem. We also have to define another isomorphism which operates on the trace space of the currents.

The normal trace of the currents belongs in the space $H^{-1/2}(\partial K)$ (the dual space of $H^{1/2}(\partial K)$). In fact, the isomorphism on $H^{-1/2}(\partial K)$ is induced by the isomorphism **G** using the divergence theorem. At every function $\hat{\mu}^*: H^{-1/2}(\partial\hat{K}) \to \mathbb{R}$, we associate a new function defined by:

$$\mu^* = \overline{\mathbf{G}}(\hat{\mu}^*) = \frac{1}{J_n}\hat{\mu}^* \circ F^{-1}: \partial K \to \mathbb{R} \tag{8}$$

Furthermore, we have the following duality identity in the trace spaces:

$$\left\langle \overline{\mathbf{G}}(\hat{\mu}^*), \hat{\mu} \circ F^{-1} \right\rangle_{H^{-1/2}(\partial K), H^{1/2}(\partial K)} = \left\langle \hat{\mu}^*, \hat{\mu} \right\rangle_{H^{-1/2}(\partial\hat{K}), H^{1/2}(\partial\hat{K})} \tag{9}$$

2.1.2 The reference mixed dual variational formulation

The previous isomorphisms are defined locally on each of the elements. The question now is: how can this local isomorphism be extended to global spaces $L^2(\Omega)$ and $H(div,\Omega)$? This can be done by writing the transmission condition on the element interfaces. For instance, if we look at the solution $\vec{p} \in H(div,\Omega)$, it means that $\vec{p}.\vec{n}$ is continuous through the interfaces. From the isomorphism $\overline{\mathbf{G}}$ defined previously, we deduce that $\frac{1}{J_n}\hat{\vec{p}}.\hat{\vec{n}}$ should be continuous in the reference geometry. By denoting $\hat{\Gamma}_i = \bigcup_{\partial K \subset \Gamma_i} G(\partial K)$, we obtain the two global spaces on the reference domain (for flux and current):

$$L^2(\hat{\Omega}) \text{ and } \hat{W}_{0,\hat{\Gamma}_2}(\hat{\Omega}) = \left\{ \hat{\vec{q}} : \hat{\vec{q}}_{/\hat{K}} \in H\left(div,\hat{K}\right); \frac{1}{J_n}\hat{\vec{q}}.\hat{\vec{n}} \textit{ continuous } ; \hat{\vec{q}}.\hat{\vec{n}} = 0 \textit{ on } \hat{\Gamma}_2 \right\}$$

It's important to note that most of the finite elements are such that the transformation F leads to a Jacobian J_n which is continuous through the element interfaces, thus the continuity condition of $\frac{1}{J_n}\hat{\vec{p}}.\hat{\vec{n}}$ is equivalent to the continuity condition of $\hat{\vec{p}}.\hat{\vec{n}}$ and thus, the space $\hat{W}_{0,\hat{\Gamma}_2}(\hat{\Omega})$ is identical to space $H_{0,\hat{\Gamma}_2}(div,\hat{\Omega})$. Using a change of variable and the previous local isomorphisms, the variational formulation can be written in the reference geometry:

Find $(\hat{\vec{p}},\hat{\phi}) \in \hat{W}_{0,\hat{\Gamma}_2}(\hat{\Omega}) \times L^2(\hat{\Omega})$ such that:

$$\begin{cases} \sum_{K\in T_h} \left\{ \frac{1}{D_K} \int_{\hat{K}} (M_K \hat{\vec{p}}).\hat{\vec{q}} d\hat{x} - \int_{\hat{K}} \hat{\phi} \vec{\nabla}.\hat{\vec{q}}\, d\hat{x} \right\} + \sum_{\partial K \cap \Gamma_3} \frac{1}{\tau_K} \int_{\partial \hat{K}} \frac{(\hat{\vec{p}}.\hat{\vec{n}})(\hat{\vec{q}}.\hat{\vec{n}})}{J_n^K} d\hat{\gamma} = 0 \quad \forall \hat{\vec{q}} \in \hat{W}_{0,\hat{\Gamma}_2}(\hat{\Omega}) \\ \sum_{K\in T_h} \left\{ -\int_{\hat{K}} \vec{\nabla}.\hat{\vec{p}}\,\hat{\psi}\, d\hat{x} - \Sigma^K \int_{\hat{K}} \hat{\phi}\hat{\psi} J_K d\hat{x} \right\} = \sum_{K\in T_h} \left\{ -\int_{\hat{K}} \hat{S}\hat{\psi} J_K d\hat{x} \right\} \quad \forall \hat{\psi} \in L^2(\hat{\Omega}) \end{cases} \tag{10}$$

With: $$M_K = \frac{1}{J_K} (DF_K)^T DF_K \tag{11}$$

Finally, by giving a partition of the domain and a transformation F defined on each sub-domain, the problem is reduced to calculation of matrix M and the two Jacobians J and J_n.

2.2 Mixed methods over convex quadrilaterals

In this chapter we shall introduce the RTN finite element family which is the most conventional approximation of $H(div)$ for rectangular geometry. For the sake of simplicity, we consider below the 2D case only, thus the reference element is $[0,1]\times[0,1]$. The flux which belongs in $L^2(\hat{K})$ is approximated in $Q_{k-1,k-1}(\hat{K})$, while the current which belongs in $H(div,\hat{K})$ is represented in $D_k(\hat{K}) = \left[Q_{k,k-1}(\hat{K}) \times \{0\}\right] \oplus \left[\{0\} \times Q_{k-1,k}(\hat{K})\right]$,

thus the d^{th} component of the current belongs in the polynomial space of degree k for the variable associated with direction d and degree k-1 for the others.
In order to minimize the non zero terms of the matrices, it is useful to choose an orthogonal basis of the $Q_{k-1,k-1}(\hat{K})$ space. This can be done via products of 1D Lagrange polynomials where the Lagrange nodes are located at the Gauss-Legendre points (Lautard, 1993).
The discrete spaces induced by the RTN finite elements RT_{k-1} on the computational domain triangulated by quadrilaterals are:

$$V_h^k = \left\{ \psi_h \in L^2(\Omega) : \psi_{h/K} \circ F \in Q_{k-1,k-1}(\hat{K}) \ \ \forall K \in \mathrm{T_h} \right\} \tag{12}$$

$$W_h^k = \left\{ \vec{q}_h \in H_{0,\Gamma_2}(div,\Omega) : J\,(DF)^{-1} \vec{q}_{h/K} \circ F \in D_k(\hat{K}) \ \ \forall K \in \mathrm{T_h} \right\} \tag{13}$$

It can be seen that spaces V_h^k and W_h^k are not necessarily piecewise polynomials. This depends on the choice of the mapping F.
The discrete problem consists in finding functions $(\vec{p}_h, \varphi_h) \in W_h^k \times V_h^k$ such that:

$$\begin{cases} \displaystyle\sum_{K \in \mathrm{T_h}} \left\{ \frac{1}{\mathrm{D}_K} \int_K \vec{p}_h . \vec{q}_h dx - \int_K \phi_h \, div\, \vec{q}_h \, dx + \frac{1}{\tau_K} \int_{\partial K \cap \Gamma_3} (\vec{p}_h . \vec{n})(\vec{q}_h . \vec{n}) d\gamma \right\} = 0 \quad \forall \vec{q}_h \in W_h^k \\ \displaystyle\sum_{K \in \mathrm{T_h}} \left\{ - \int_K div\, \vec{p}_h \, \psi_h dx - \Sigma^K \int_K \phi_h \psi_h dx \right\} = \sum_{K \in \mathrm{T_h}} \left\{ - \int_K S \psi_h dx \right\} \qquad \forall \psi_h \in V_h^k \end{cases} \tag{14}$$

Assuming that F is a C^1-difféomorphism, the equivalent problem in the reference geometry is:

Find $(\hat{\vec{p}}_h, \hat{\phi}_h) \in \hat{W}_h^k \times \hat{V}_h^k$ such that:

$$\begin{cases} \displaystyle\sum_{K \in \mathrm{T_h}} \left\{ \frac{1}{\mathrm{D}_K} \int_{\hat{K}} (M_K \hat{\vec{p}}_h) . \hat{\vec{q}}_h d\hat{x} - \int_{\hat{K}} \hat{\phi}_h \, \hat{\nabla} . \hat{\vec{q}}_h \, d\hat{x} + \frac{1}{\tau_K} \int_{\partial K \cap \Gamma_3} \frac{(\hat{\vec{p}}_h . \hat{\vec{n}})(\hat{\vec{q}}_h . \hat{\vec{n}})}{J_n^K} d\hat{\gamma} \right\} = 0 \quad \forall \hat{\vec{q}}_h \in \hat{W}_h^k \\ \displaystyle\sum_{K \in \mathrm{T_h}} \left\{ - \int_{\hat{K}} \hat{\nabla} . \hat{\vec{p}}_h \, \hat{\psi}_h \, d\hat{x} - \Sigma^K \int_{\hat{K}} \hat{\phi}_h \hat{\psi}_h \, J_K d\hat{x} \right\} = \sum_{K \in \mathrm{T_h}} \left\{ - \int_{\hat{K}} \hat{S} \hat{\psi}_h J_K d\hat{x} \right\} \qquad \forall \hat{\psi}_h \in \hat{V}_h^k \end{cases} \tag{15}$$

where:

$$\hat{V}_h^k = \left\{ \hat{\psi}_h \in L^2(\hat{\Omega}) : \hat{\psi}_{h/\hat{K}} \in Q_{k-1,k-1}(\hat{K}) \ \ \forall \hat{K} \in \mathrm{T_h} \right\} \tag{16}$$

$$\hat{W}_h^k = \left\{ \hat{\vec{q}}_h \in L^2(\hat{\Omega})^d : \hat{\vec{q}}_{h/\hat{K}} \in D_k(\hat{K}) \, ; \frac{1}{J_n^K} \hat{\vec{q}}_h . \hat{\vec{n}}_{\hat{K}} \ continuous \, ; \hat{\vec{q}}_h . \hat{\vec{n}}_{\hat{K}} = 0 \ on \ \hat{\Gamma}_2 \right\} \tag{17}$$

In the case where the condition "$\frac{1}{J_n^K} \hat{\vec{q}}_h . \hat{\vec{n}}_{\hat{K}}$ continuous" is difficult to fulfil in the space $\hat{W}_h^k$, this condition can be forced via Lagrange multipliers (mixed hybrid dual formulation).

3 The case of rectangular geometry

In rectangular geometry, the RTN elements have the interesting property of producing sparse matrices with coupling terms oriented only along the axis. This property is a consequence of the elementary mappings which are homothety (the matrix M is thus diagonal). Therefore the orthogonal property of the basis is kept in the computational domain.

3.1 The matrix system

The unknowns are ordered so that the x, y and z components of current unknown are numbered first and the unknowns corresponding to the flux afterwards. After some mathematical manipulations, we obtain the following system:

$$\begin{bmatrix} -A_x & 0 & 0 & B_x \\ 0 & -A_y & 0 & B_y \\ 0 & 0 & -A_z & B_z \\ B_x^T & B_y^T & B_z^T & T \end{bmatrix} \begin{bmatrix} p_x \\ p_y \\ p_z \\ \varphi \end{bmatrix} = \begin{bmatrix} 0 \\ 0 \\ 0 \\ S \end{bmatrix} \tag{18}$$

B_d $(d = x, y, z)$ is a rectangular matrix coupling the flux and the current components. These matrices can be reduced to 'difference' matrices by a particular choice of the polynomial bases of the current. Also if an orthogonal basis is chosen on the flux basis, A_d are block diagonal matrices and T is a diagonal matrix.

It has been established numerically that using reduced integration instead of exact integration can improve the discrete solution. This property is linked to what is known as a super-convergence property. The best choice is a Gaussian quadrature of an order below the one which gives an exact integration (Order $2k+1$ for RTN elements of degree k).

3.2 The iterative algorithm

In order to obtain a positive definite matrix, the flux is substituted into the current equations (this is very easy because T is diagonal). We obtain the current equation below:

$$\begin{pmatrix} W_x & B_x T^{-1} B_y^T & B_x T^{-1} B_z^T \\ B_y T^{-1} B_x^T & W_y & B_y T^{-1} B_z^T \\ B_z T^{-1} B_x^T & B_z T^{-1} B_y^T & W_z \end{pmatrix} \begin{pmatrix} p_x \\ p_y \\ p_z \end{pmatrix} = \begin{pmatrix} B_x T^{-1} S \\ B_y T^{-1} S \\ B_z T^{-1} S \end{pmatrix} \tag{19}$$

where $W_d = A_d + B_d T^{-1} B_d^T \quad ; d = x, y \text{ ou } z$

Using the directional leakage $J_d = B_d^T \, p_d$, we perform a block Gauss-Seidel algorithm, each block corresponding to one of the three components of the current vectors (Lautard, 1993). This algorithm can be viewed as an alternating direction sweep. If we consider a direction d, our particular choice of the RTN basis produces in the graph of W_d only connection oriented along the d axis. If the nodes are numbered along direction d first, the matrix W_d becomes block diagonal (each block being associated to a line of nodes), thus resolution can be obtained very effectively on vector computers, because each of the subsystems can be solved simultaneously. At the end of the sweep, the even flux is updated and used to recalculate a new source.

4 The treatment of hexagonal geometry

We give a reminder here of the method suggested by Chao and Tsoulfanidis (1995) for nodal approximation. The idea was to split the hexagon into 4 trapezes and use a conformal mapping from a trapezoid to a rectangle. In the context of mixed methods, the main difficulty lies in the fact that while the transformation is a conformal mapping on each trapezoid separately, it is not conformal on the whole domain. At an oblique interface of two trapezoids, the Jacobian is discontinuous. Moreover, a point on an interface has two different images according to the hexagon being considered (Lautard, 1999). These transmission conditions are difficult to be fulfil in the discrete polynomial space. The best solution is therefore to introduce Lagrange multipliers and then to use a mixed hybrid dual finite element approximation. All of this makes this method very complicated to implement in the MINOS rectangular solver.

We now go on to present three methods which were motivated by the Chao method. We restrict our presentation to 2D since it can be extended to three dimensions can be done without difficulty. The first method consists in splitting the hexagon into 4 trapezoids and using a bilinear mapping on each trapezoid as proposed by Hennart and Mund (1997) in the context of a nodal method. The next two methods are new approaches and consist in splitting the hexagon into 3 lozenges, using either an affine mapping or a conformal mapping from the lozenges to a rectangle domain. The main advantage here is that each lozenge can be easily split into smaller lozenges, so there is no difficulty in obtaining convergence in space. Another advantage is that this splitting preserves the fundamental symmetries of the hexagonal geometry.

4.1 Splitting into trapezoids with bilinear mapping (TBI)

In this method, we split a hexagon into 4 trapezoids. By transforming each trapezoid into a rectangle, we obtain a geometry which can be directly treated by the rectangular solver by sweeping of the two rectangular directions x and y (Figure 1). This is a distinct advantage for fast implementation in the MINOS solver.

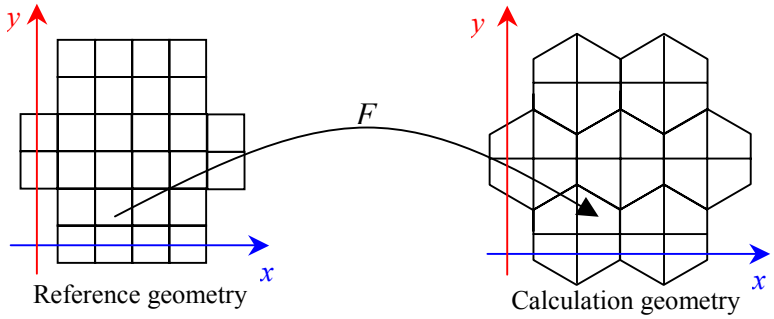

Figure 1 – Hexagonal geometry with splitting into trapezes

If we consider the right upper quarter trapezoid, the coordinate transformation, the Jacobian matrix and the Jacobian read:

$$F(\hat{x},\hat{y}) = \begin{pmatrix} x(\hat{x},\hat{y}) \\ y(\hat{x},\hat{y}) \end{pmatrix} = \begin{pmatrix} \hat{x} \\ \frac{2}{\sqrt{3}}\hat{y} - \frac{1}{\sqrt{3}}\hat{x}\hat{y} \end{pmatrix} \qquad DF = \begin{pmatrix} 1 & 0 \\ -\frac{\hat{y}}{\sqrt{3}} & \frac{2-\hat{x}}{\sqrt{3}} \end{pmatrix} \qquad J = \left|\det(DF)\right| = \frac{2-\hat{x}}{\sqrt{3}}$$

The matrix coupling reads:

$$M = \frac{1}{J} DF^T DF = \frac{1}{\sqrt{3}} \begin{pmatrix} \frac{3+\hat{y}^2}{2-\hat{x}} & -\hat{y} \\ -\hat{y} & 2-\hat{x} \end{pmatrix} \tag{20}$$

This transformation nevertheless has the disadvantage of producing cross-derivatives in the transformed operator because the matrix M is full.

By replacing M and J in the discrete form, we obtain the equation associated with the TBI (Trapeze and BIlinear) transformation. Moreover, the calculation of J_n shows that it stays constant and continuous along the different edges, thus the transmission conditions associated with the transformed operator correspond to the continuity of the normal trace and the mixed dual approximation applies without Lagrange multipliers.

Therefore, we can use the same iterative algorithm as the one in the MINOS solver. The only difference is that at each iteration, we have to add a contribution to the source term coming from the transverse coupling.

$$\begin{pmatrix} W_x & B_x T^{-1} B_y^T \\ B_y T^{-1} B_x^T & W_y \end{pmatrix} \begin{pmatrix} p_x \\ p_y \end{pmatrix} = \begin{pmatrix} B_x T^{-1} S \\ B_y T^{-1} S \end{pmatrix} - \begin{pmatrix} 0 & C_{xy} \\ C_{xy}^T & 0 \end{pmatrix} \begin{pmatrix} p_x \\ p_y \end{pmatrix} \tag{21}$$

where C_{xy} is the matrix coupling the components of the current.

This method has been implemented in MINOS and is satisfactory, the main disadvantage is that we cannot divide the trapezoid into smaller trapezoidal elements and thus perform a mesh convergence.

4.2 Splitting into lozenges

The main feature of splitting into lozenges is that two elements adjacent to a third element K can be adjacent. This property implies that the reference geometry formed by square elements does not form a pavement of the plane. In fact, the reference geometry can be viewed as a polyedric surface in $\mathbb{R}^3$; in the 2D plane, we can just have a projected view (Figure 2). In this figure, the elements are connected along lines that we denote by u, v and w. The natural symmetry of the hexagonal geometry is thus conserved.

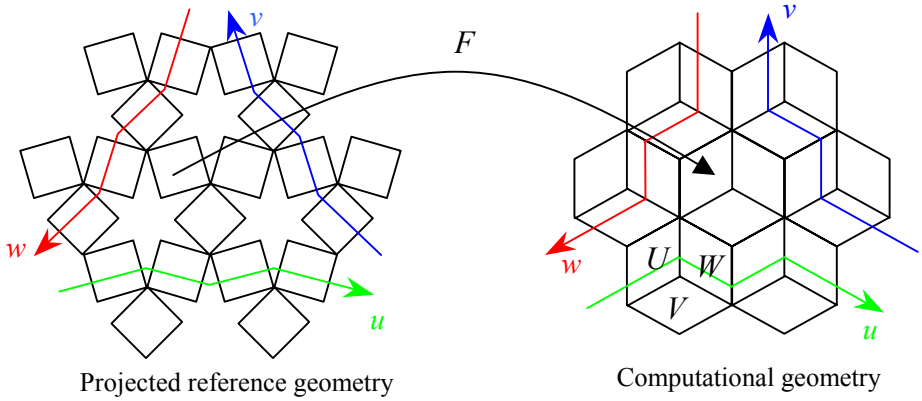

Figure 2 – Sweeping directions on hexagonal geometry with lozenges

4.2.1 Affine mapping on lozenges (LAF)

If we take lozenge *U* (Figure 2) of side *R* as an example, we easily obtain:

$$F_U(\hat{x},\hat{y}) = \begin{pmatrix} x(\hat{x},\hat{y}) \\ x(\hat{x},\hat{y}) \end{pmatrix} = \frac{R}{2}\begin{pmatrix} \sqrt{3}\,(\hat{x}-1) \\ (\hat{x}+2\hat{y}-1) \end{pmatrix} \quad ; \quad DF_U = \frac{R}{2}\begin{pmatrix} \sqrt{3} & 0 \\ 1 & 2 \end{pmatrix} \tag{22}$$

The other mappings derive from the previous mapping by rotations ($2\pi/3$ for lozenge *V* and $4\pi/3$ for lozenge *W*). The Jacobian and the matrix *M* are the same for each lozenge and can be expressed thus:

$$J = R^2\,\frac{\sqrt{3}}{2} \text{ and } M = \frac{1}{\sqrt{3}}\begin{pmatrix} 2 & 1 \\ 1 & 2 \end{pmatrix} \tag{23}$$

The surface Jacobian J_n is equal to the ratio between the length of the side of the reference square and the length of the side of its image, thus $J_n = R$, and remains constant and continuous through the interfaces. The space $\hat{W}_{0,\hat{\Gamma}_2}(div,\hat{\Omega})$ is thus identical to $H_{0,\hat{\Gamma}_2}(div,\hat{\Omega})$ and the RTN discrete spaces can be used as in the rectangular geometry.

Since matrix *M* is constant in space, the coupling terms between currents are easy to compute. By eliminating the flux unknowns, we obtain a new matrix system on the current components:

$$\begin{pmatrix} W_u & B_uT^{-1}B_v^T & B_uT^{-1}B_w^T \\ B_vT^{-1}B_u^T & W_v & B_vT^{-1}B_w^T \\ B_wT^{-1}B_u^T & B_wT^{-1}B_v^T & W_w \end{pmatrix}\begin{pmatrix} p_u \\ p_v \\ p_w \end{pmatrix} = \begin{pmatrix} B_uT^{-1}S \\ B_vT^{-1}S \\ B_wT^{-1}S \end{pmatrix} - \begin{pmatrix} 0 & C_{uv} & C_{wu}^T \\ C_{uv}^T & 0 & C_{vw} \\ C_{wu} & C_{vw}^T & 0 \end{pmatrix}\begin{pmatrix} p_u \\ p_v \\ p_w \end{pmatrix} \tag{24}$$

where $W_d = A_d + B_dT^{-1}B_d^T$; $d = u, v, w$

The iterative procedure is close to that for the rectangular case, the only exception being that we have three sweeping directions and a supplementary iteration to take in account the coupling terms between the current components. One of the advantages of this method is that it is easy to reduce the space meshing by subdividing each lozenge into smaller lozenges. This is shown in Figure 3.

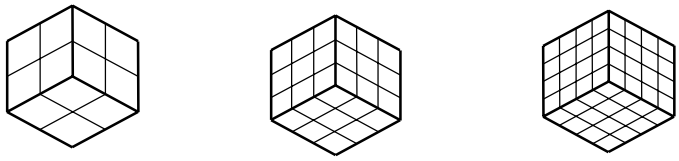

Figure 3 – Different ways of splitting up a hexagon

4.2.2 Conformal mapping (LSC)

A third method can be carried out by using conformal mapping of the unite square into the lozenge. For this, we use the Schwarz-Christoffel transformation (Marukevitch, 1967). The Schwarz-Christoffel transformation is a particular conformal mapping which maps the half complex upper plane into an arbitrary convex *n*-gone; the general expression reads:

$$T(r) = C\int_0^r (t-a_1)^{\theta_1-1}...(t-a_n)^{\theta_n-1}\,dt \quad ; r \in \mathbb{C}^+ \tag{25}$$

where C is a positive constant, $a_1 <...< a_n \in \mathbb{R}$ are constants which depend on the position of the vertex ($n=4$ and $a_1 = -k', a_2 = -1, a_3 = 1, \ a_4 = k'$ for a symmetric quadrangular) and $\theta_i\pi$ are the angles of the polygon ($\theta_1 = \theta_2 = \theta_3 = \theta_4 = 1/2$) for a square and $\theta_1 = \theta_3 = 1/3,\ \theta_2 = \theta_4 = 2/3$ for a lozenge). Therefore the conformal mapping F from the lozenge into a rectangle is the composition of two conformal mappings.

After some mathematical developments, we obtain $k' = 3 + 2\sqrt{2}$.

The Jacobian J, J_n and the matrix M read:

$$J(r) = 0{,}8972892\left|\frac{(r-1)\,(r+k')}{(r+1)\,(r-k')}\right|^{\frac{1}{3}} \ ; r \in \mathbb{C}^+ \ , \ J_n = \sqrt{J} \text{ and } M = Identity$$

The complex variable r is expressed in terms of elliptic function by $r = sn(\hat{x} + i\hat{y}, k'^2)$.

The Jacobian is space-dependent and has singularities at the vertices corresponding to the acute angles of the lozenge. In this case, we have extended the variational formulation by using weighted Sobolev spaces (Schneider, 2000).

It can be observed that J_n is continuous and we have no jump in contour lines at these interfaces as we did with conformal mapping on trapezes. Thus, the space $\hat{W}_{0,\Gamma_2}(\hat{\Omega})$ corresponds to the space $H_{0,\Gamma_2}(div, \hat{\Omega})$. As a result, the standard mixed dual variational formulation applies without difficulty. Nevertheless, the property (J_n continuous through the interfaces) is lost if the partitions of a hexagon are made as shown in Figure 3. The only possible refining is a 2×2 as shown in Figure 4.

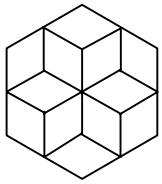

Figure 4 – 2×2 partition associated with conformal mapping

Finally, the matrix system is slightly simpler than that obtained with affine transformation since we do not have the coupling transverse matrices C (Eq. (24)). The difficulty arises because J is space-dependent and is not expressed as a tensorial product of 1D functions, thus T is no longer a diagonal matrix but a block diagonal matrix. The fill in of the matrix T produces a fill in of the matrices W_d. To avoid this difficulty, we use a Gauss-Legendre quadrature formula to compute the T entries.

5 Extension to pin-by-pin calculation

We have described a numerical method which uses discretization based on repetitive hexagons. This geometric configuration is well suited to homogenized problems where the entire assembly has been homogenized. To be more exhaustive, we have to examine the

configuration produced by pin-by-pin homogenization. In this case, as shown in Figure 5, we have to take into account the inter assembly region, where the regular space meshing is slightly destroyed due to the presence of the assembly boxes. The homogenized pin-by-pin core configuration is represented by the dotted lines in Figure 5. As can be shown, two supplementary element shapes add to the standard regular hexagons (a,a,a,a,a,a). They are symbolized by the coding (a,b,a,b,a,b) and (a,a,b,a,a,b). Extension of the methods described in Section 4 has been studied recently and this extension will be implemented soon in the MINOS solver.

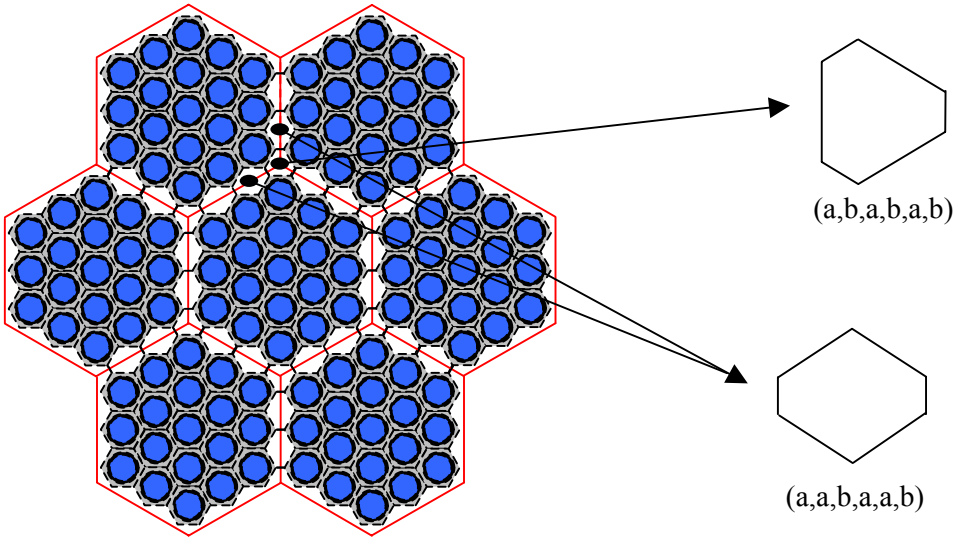

Figure 5 – Unstructured hexagonal geometry

The LAF and TBI methods can be extended to this pin-by-pin calculation without difficulty, unlike the LSC method. As a matter of fact, the conformal mapping produces jumps of the Jacobian at the interfaces, which are impossible to take into account. The different splittings of the elements are given in Figure 6 for the TBI method and Figure 7 for the LAF method. It can be seen that the TBI method needs the construction of 5 new different elements (which differ by their affine mapping), whereas the LAF method needs only 2 new different elements.

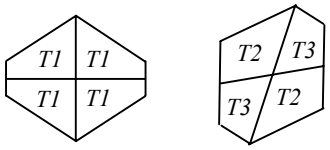

Splitting of hexagons (a,a,b,a,a,b)

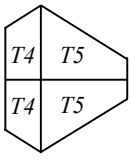

Splitting of hexagons (a,b,a,b,a,b)

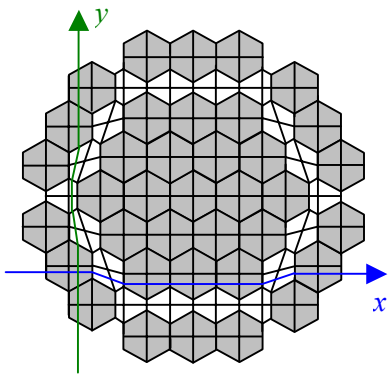

Figure 6 – Finite element mesh for the TBI method and new finite elements

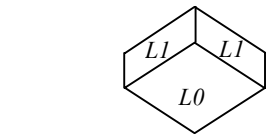

Splitting of hexagons (a,a,b,a,a,b)

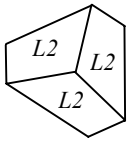

Splitting of hexagons (a,b,a,b,a,b)

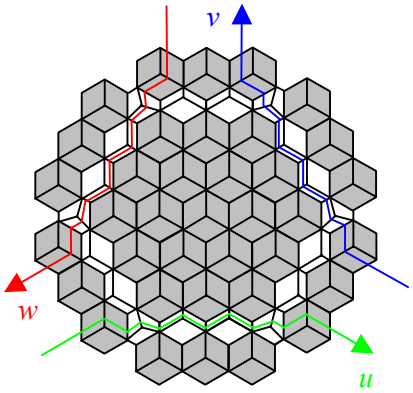

Figure 7 – Finite element mesh for the LAF method and new finite elements

6 Numerical application

The previous methods have been compared on the two-group IAEA benchmark problem extended to hexagonal geometry (Hennart, 1997). We describe here only the results of the case with radial reflector included and an albedo boundary condition on the outer surfaces $\tau = 0.5$. The other three configurations give similar results (Schneider, 2000). The core map and the cross-sections are given in Figure 8.

Material	**1**	**2**	**3**	**4**
D_1	1.5	1.5	1.5	1.5
D_2	0.4	0.4	0.4	0.4
$\Sigma_{a1} + \Sigma_{12}$	0.03	0.03	0.03	0.04
Σ_{a2}	0.08	0.085	0.13	0.01
Σ_{12}	0.02	0.02	0.02	0.04
$\nu\Sigma_{f1}$	0	0	0	0
$\nu\Sigma_{f2}$	0.135	0.135	0.135	0

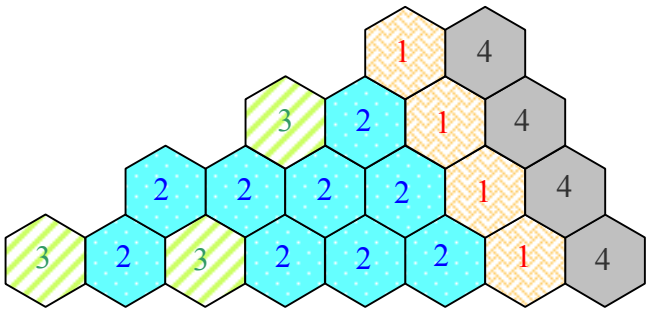

Figure 8 – Configuration of the modified IAEA 2D Hexagonal Benchmark (with reflector)

Table 1 gives the discrepancy with respect to the reference of the k_{eff} (in bold) and the computing time (in italics). The columns correspond to various mesh sizes (when it's possible) and the lines to various degrees.

As shown, the TBI and LAF methods converge correctly. The TBI method converges slightly better than the LAF method (in degrees) but is more time-consuming. The results obtained with the LAF method show that increasing the degree of approximation is more efficient than reducing the mesh size (in terms of computing time). Another observation is that the LSC method converges slowly. This is probably due to the singularity of the Jacobian which leads to a slowly converging numerical quadrature.

Mesh / Degree	TBI M1	LAF M1	LAF M2	LAF M3	LSC M1	LSC M2
1 (RT0)	**-61** *0.18*	**-106** *0.09*	**-7** *0.15*	**-4** *0.48*	**-139** *0.02*	**-79** *0.10*
2 (RT1)	**-4** *0.33*	**+9** *0.17*	**0** *1.08*	**0** *3.03*	**-163** *0.12*	**-100** *1.18*
3 (RT2)	**0** *1.36*	**-1** *0.69*	**0** *3.89*	**0** *12.15*	**-39** *0.54*	**-12** *4.75*
4 (RT3)	**0** *3.27*	**0** *1.90*	**0** *10.92*	**0** *31.90*	**-12** *2.08*	**-1** *21.93*

Table 1 – Error **ε** (in pcm) and computing time *t (in seconds on HP-B1000 W.S.)* for the modified IAEA 2D Hexagonal Benchmark. $\varepsilon = 10^5\left(k_{eff} - k_{eff}^{ref}\right)$, ($k_{eff}^{ref} = 1.00551$)

Next, we compared the results of our old method used in CRONOS and based on primal finite elements (PRIAM). Table 2 gives the power distribution obtained by PRIAM with a cubic finite element and a mesh 2 for space discretization. This calculation has been taken as a reference. Table 3 gives the assembly power density for the 3 MINOS methods with respect to the CRONOS reference calculation. As shown, the three methods give good results, those obtained with the LAF method being slightly better.

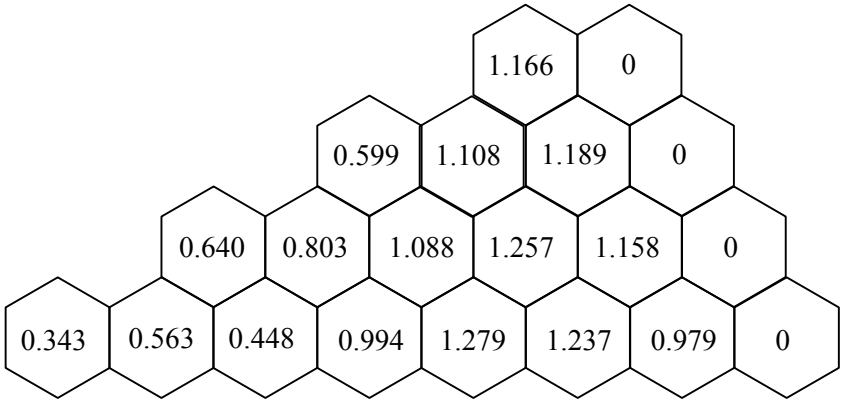

Table 2 – The Cronos reference power density

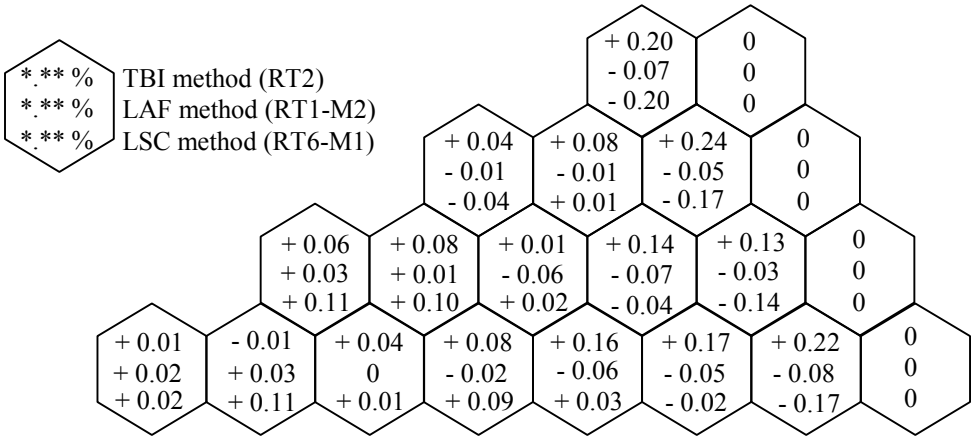

Table 3 – Absolute errors in % of the power density

The next table (Table 4) shows the speed-up achieved with the new MINOS methods with respect to the standard CRONOS calculations based on primal finite elements. The CRONOS calculations were carried out with various degrees and mesh sizes. The MINOS calculation is the one which gives about the same error on the k_{eff} as CRONOS. As shown, we get a factor greater than 10 in all the calculations.

	Type E.F. (error with k_{eff}^{ref})	Parabolic-Mesh2 (5 pcm)	Parabolic-Mesh3 (1 pcm)	Cubic-Mesh2 (reference)
LAF	RT1-Mesh1 (9 pcm)	**23**		
	RT2-Mesh1 (1 pcm)		**26**	**33**
	RT1-Mesh2 (reference)		**16**	**21**
TBI	RT1-Mesh1 (4 pcm)	**12**		
	RT2-Mesh1 (reference)		**13**	**17**

Table 4 – Computing time ratio between CRONOS, LAF and TBI for equivalent k_{eff} error

7 Conclusion

For Cartesian geometry and for the treatment of the diffusion equation, among the different finite element methods, the mixed dual approximation using Raviart-Thomas-Nedelec elements gives fast results with good vectorization. In this paper, we have introduced the general framework of its extension to quadrangular unstructured geometry. This general context has been applied for the treatment of regular hexagonal geometry. Different ways of splitting the hexagons and different elementary mappings have been examined. The numerical results show that splitting the hexagon into three lozenges and using an affine mapping gives better results. A gain of a factor of about 20 has been achieved with respect to the conventional finite elements. Moreover, this method can be easily extended to perform pin-by-pin calculations. Nevertheless, splitting into trapezes has the advantage of being rapidly implemented in the existing rectangular solver. These good results encourage us to pursue the work and extend this method for the treatment of the transport SPN calculations on arbitrary quadrangular unstructured meshes.

8 Acknowledgments

The developments relating to the hexagonal geometry were made with the support of Framatome and we thank L. Paillard for his valuable help.

9 References

[Baudron 2001] A.M. Baudron, J.J. Lautard, La méthode Minos. Approximation par des éléments mixtes duaux des équations PN simplifiées pour l'opérateur du transport – Note CEA (To appear)

[Brezzi 1991] F. Brezzi, M. Fortin, Mixed and Hybrid Finite Element Methods, Springer Verlag (1991).

[Ciarlet 1991] P.G. Ciarlet and P.L. Lions, Handbook of Numerical Analysis, North Holland (1991).

[Chao 1995] Y.A. Chao N. Tsoulfanidis, Conformal Mapping and Hexagonal Nodal Methods Mathematical Foundation, Nucl. Sci. Eng. 121, p.210 (1995).

[Hennart 1997] J.P. Hennart E.H. Mund and E. Del Valle, A Composite Nodal Finite Element for Hexagons, Nucl. Sci. Eng. 127, p.139 (1997).

[Lautard 1990] J.J. Lautard, S. Loubiere, C. Fedon-Magnaud, CRONOS a Modular Computational System for Neutronic Core Calculations, Specialist IAEA meeting. Advanced Calculational Methods for Power Reactors, Cadarache, France (1990).

[Lautard 1993] J.J. Lautard F. Moreau, A fast 3D parallel solver based on the mixed dual finite element approximation, Proc. ANS Topical Mtg., Mathematical Methods and supercomputing in Nuclear Applications, Karlsruhe, Germany, (1993).

[Lautard 1994] J.J. Lautard, La méthode nodale de CRONOS : MINOS, Approximation par des éléments mixtes duaux, Note C.E.A-N- 2763 (1984).

[Lautard 1999] J.J. Lautard, D. Schneider, A.M. Baudron, Mixed Dual Methods for Neutronic Reactor Core Calculation in the CRONOS System, Proc. ANS Topical Mtg., Mathematics and Computation, Reactor Physics and Environmental Analysis in Nuclear Applications, Volume 1, Madrid, Spain, (1999).

[Lewis 1985] E.E. Lewis, W.F. Miller, Computational Methods of Neutron Transport, Wiley-Interscience Publication (1985).

[Markushevich 1967] A.I. Markushevich, Theory of functions of a complex variable, Prentice-Hall (1967).

[Palmiotti 1993] G. Palmiotti, C.B. Carrico, E.E. Lewis, Variational Nodal Transport methods with anisotropic scattering, Nucl. Sci. Eng., 115 (1993).

[Raviart 1977] P.A. Raviart, J.P. Thomas, A Mixed Finite Element Method for the 2nd elliptic problems, Mathematical Aspects of the Finite Element Method. Lecture Notes in Mathematics 606, Springer Verlag (1977).

[Roberts 1989] J.E. Roberts, J.M. Thomas, Mixed and hybrid methods, Handbook of Numerical Analysis, P.G. Ciarlet and J.L. Lions Eds, Vol II, Parts 1 North Holland, Amsterdam (1989).

[Schneider 2000] D. Schneider, Eléments finis mixtes duaux pour la résolution numérique de l'équation de la diffusion neutronique en géométrie hexagonale, Thèse de Doctorat Paris VI, (2000).